Hynninen, Teemu; Heinonen, Vili; Dias, Christian L.; Karttunen, Mikko; Foster, Adam S.; Ala-Nissila, Tapio

# Cutting Ice: Nanowire regelation

P H Y S I C A L   R E V I E W   L E T T E R S

# Cutting Ice: Nanowire Regelation

Teemu Hynninen,[1,2,*] Vili Heinonen,[2] Cristiano L. Dias,[3,4] Mikko Karttunen,[3] Adam S. Foster,[1,2] and Tapio Ala-Nissila[2,5]

[1]*Department of Physics, Tampere University of Technology, P.O. Box 692, FI-33101 Tampere, Finland*
[2]*Department of Applied Physics, Aalto University School of Science and Technology, P.O. Box 11100, FI-00076 Aalto, Espoo, Finland*
[3]*Department of Applied Mathematics, The University of Western Ontario, London, Ontario, Canada N6A 5B7*
[4]*Department of Biochemistry, University of Toronto, Toronto, Ontario, Canada M5S 1A8*
[5]*Department of Physics, Brown University, Providence Rhode Island 02912-1843, USA*

Even below its normal melting temperature, ice melts when subjected to high pressure and refreezes once the pressure is lifted. A classic demonstration of this regelation phenomenon is the passing of a thin wire through a block of ice when sufficient force is exerted. Here we present a molecular-dynamics study of a nanowire cutting through ice to unravel the molecular level mechanisms responsible for regelation. In particular, we show that the transition from a stationary to a moving wire due to increased driving force changes from symmetric and continuous to asymmetric and discontinuous as a hydrophilic wire is replaced by a hydrophobic one. This is explained at the molecular level in terms of the wetting properties of the wire.

Melting and freezing of water are among the most important phase transitions in nature. Not only does the amount of ice on the planet regulate global sea levels, melting ice plays a part in phenomena as diverse as the electrification of thunderclouds, frost heave, and slippery ice surfaces [1,2]. Early studies concluded that ice melts under moderate pressures, forming a thin water layer that is the source of ice's slipperiness. The idea of pressure melting explaining ice friction has remained as common wisdom; however, it was already disputed upon publication by Faraday and Gibbs [3,4]. Later studies have confirmed that the pressures required are much too high for standard slippery scenarios, and ice friction is dominated by the spontaneous formation of a liquid-like premelt layer on the ice surface even well below freezing temperature [1,2]. Nonetheless, pressure melting is real and does play a role when the temperature is close to $0\,°C$ or the pressures involved are high. The phenomenon of ice melting when subject to high pressure and refreezing once the pressure is lifted, regelation, acts in systems ranging from massive glaciers, where it allows ice sheets to flow around obstacles [1,5], to Thomson's classic 19th century experiment of letting a wire pass through a block of ice [6]. Indeed, regelation is often demonstrated experimentally by setting a thin, weighted wire on a block of ice, whereby the wire slowly passes through the ice [7,8]. Such experiments show complicated motion of the wire as a function of temperature, driving force, wire diameter, and wire material, due to defects and impurities in the ice and conduction of heat through the wire [9,10]. Typically, the experimental and theoretical works on regelation have addressed the macroscopic problem. However, recent studies have emphasized how water and ice demonstrate real nanoscale phenomena in a wide variety of processes, including nucleation [11,12], adsorption [13,14], diffusion [15,16], confinement [17], and friction [18,19].

Here we study wire regelation at the nanoscale using molecular-dynamics (MD) simulations. We show that the transition from a stationary to a moving wire due to increased driving force changes from symmetric and continuous to asymmetric and discontinuous as a hydrophilic wire is replaced by a hydrophobic one. This result is explained in terms of the structure of water around the wire. In the hydrophilic case, the structure of water does not depend strongly on the driving force close to the depinning transition, as hydrophilic wires are prone to remain wet. In contrast, the structure of water around a hydrophobic wire is different for forces below and above depinning due to the energy penalty related to wetting a hydrophobic surface coupled with the asymmetry introduced by the motion of the wire. These results shed new light on our understanding of how wetting properties of materials relate to their friction on ice.

The simulations were carried out using the velocity-Verlet algorithm, as implemented in the CASHEW MD tool (an in-house code), with a time step of 1.0 fs used for numeric integration of the equations of motion. Interactions between water molecules were described using the 3D Mercedes-Benz (MB) potential, a geometric water model designed to accurately reproduce the thermodynamic and structural properties of water, including freezing and pressure-induced melting, while being computationally more efficient than, e.g., the TIPnP models [20,21]. Although the extension of the MB model to 3D is relatively new [20], in 2D the MB model has been successful in describing the correct physics of phenomena such as cold denaturation of proteins [22], water's anomalous thermodynamic properties [23], and solute hydration [24].

The parameters of the potential were scaled so as to yield a melting temperature of approximately 270 K. The temperature range of 240–280 K was probed in the simulations, the presented results being obtained at 260 K. The wire was described in a coarse grained fashion as a rigid string of beads, where the beads interact with water molecules via hard-sphere pair potentials. To mimic a hydrophilic surface, a shifted Lennard-Jones potential was used $[V(r) = 4\varepsilon\{[\sigma/(r - r_0)]^{12} - [\sigma/(r - r_0)]^6\},\ r > r_0$, with $\varepsilon = 0.03$ eV [25]]. A hydrophobic surface was produced by taking only the repulsive part of the Lennard-Jones potential. The wire was set in the $[1\bar{1}0]$ direction of the ice lattice with the wire bead separation set commensurate with the periodicity of the lattice (2.3 Å). Motion was in the [001] direction. A Langevin thermostat with a friction coefficient of the order 0.01 fs$^{-1}$ was applied to dissipate the work done on the system by the driving force. (Values in the range 0.005–0.05 fs$^{-1}$ were seen to produce qualitatively similar results.) Several schemes for driving the motion were tested. The presented simulations use a scheme where the wire is frozen in place and the surrounding ice is driven by applying a force on a layer of water molecules [26]. The velocity of the wire was determined by measuring the average velocity of the center of mass of all water molecules over 2–15 ns. The forces are reported as the total external force acting on the system, divided by the length of the wire in the simulation cell. To ensure large enough simulation volumes were used, finite size scaling of strain energy was analyzed for each wire. The simulations contained between 1000 and 10 000 water molecules.

When a nanowire is placed in bulk ice and a very weak external force is applied, it is pinned by the periodic potential of the ice lattice. In this creep regime [27–29] its motion is thermally activated as thermal energy is required to facilitate the necessary breaking of molecular bonds. When the external force exceeds a critical value $f_c$, the wire starts to move at all temperatures. This is analogous to the depinning transition, which is ubiquitous in systems such as driven overlayers, charge density waves, and vortex lattices [28–30]. In nanoregelation, depinning is due to pressure-induced melting, which is unique to ice and thus different from the yield point of solids under stress [31]. The melting is heterogeneous, occurring locally in the region of increased pressure below the wire, the surface of the wire also acting as a nucleation center.

Figure 1(a) shows the velocity of a hydrophilic wire, i.e., a wire whose surface attracts water, as a function of the driving force for three different wire radii. The critical force increases as the wire is made thicker. This is to be expected since a thick wire must push through a larger area of ice, breaking more hydrogen bonds between water molecules. Nevertheless, the force-velocity dependence and the transition itself are similar for all wire sizes. No hysteresis was seen in the simulations, suggesting the depinning transition to be a continuous one described by dynamic critical phenomena [32]; rescaling the force-velocity curves according to the estimated values for criti-
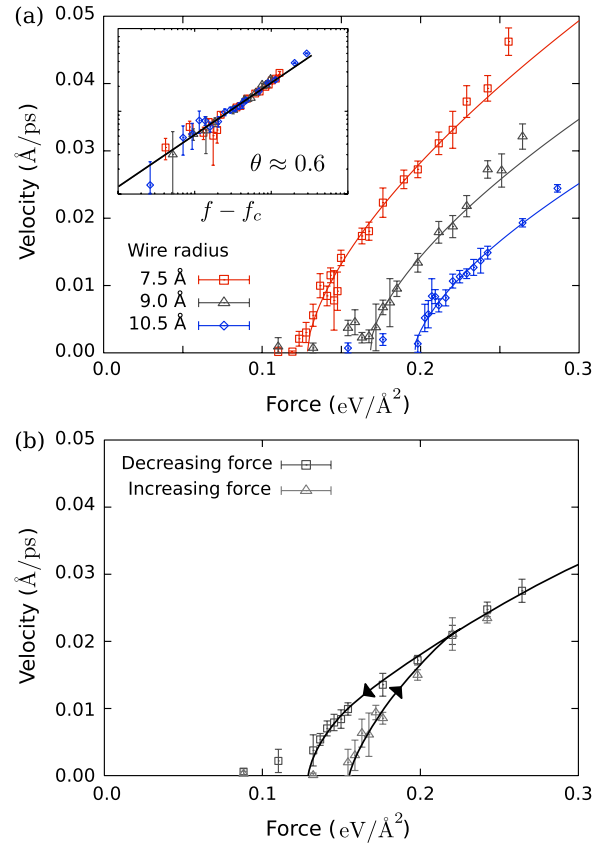


FIG. 1 (color online). (a) Velocity of a hydrophilic wire as a function of driving force for different radii. The inset shows the data on a logarithmic scale. (b) Velocity of a hydrophobic wire (9.0 Å radius) as a function of driving force.

cal forces leads to a collapse of the data on a single curve (shown on a logarithmic scale in the inset of Fig. 1). Near depinning, the motion of the wire is mainly stick-slip motion as the wire jumps from one potential minimum to the next, and the velocity seems to obey a power law of the form $v \sim (f - f_c)^\theta$. The best estimate for the critical exponent $\theta$ is 0.62 ($\pm 0.1$). Surprisingly, this value is very close to that for 2D elastic depinning (0.63) [33], although here the wire depinning is controlled by bond breaking and melting of ice.

The force-velocity correspondence of a hydrophobic wire, i.e., a wire whose surface repels water, is shown in Fig. 1(b). Again, a depinning transition is observed, but unlike in the case of the hydrophilic wire, clear hysteresis is present here: When the force is gradually increased, the depinning is seen at a higher critical force than if the force is decreased. This is an indication that the depinning transition of the hydrophobic wire is discontinuous.

As the difference between hydrophilic and hydrophobic wires is in their interaction with water molecules, the reason for the apparent difference in their depinning transitions can only be understood by analyzing the behavior of water in their surroundings. First, we examine the time-averaged liquid-solid morphology by monitoring the number and strength of hydrogen bonds the water molecules

form with each other, in the reference frame of the wire. This is measured as the ratio of the H bond potential energy and the bonding energy of an ideal four-coordinated structure [34]. Since the MB potential has tetrahedral symmetry by construction [20], such a map of bonding energy is also a probe of local tetrahedral coordination, known to distinguish solid ice and liquid water [35].

Figures 2(a) and 2(b) show the average water bonding energy around a hydrophilic wire at two different regimes: stick-slip motion just beyond the depinning [2(a)] and steady sliding at high driving force [2(b)]. Solid ice is shown as blue (dark), while liquid water is white. Clearly, the layer of liquid around the wire is very thin in both cases. The regelation tail (region above the wire where refreezing occurs) grows as the velocity of the wire increases, but this is mostly due to the finite rate of freezing. That is, a rapidly moving wire moves a longer distance before the ice behind it has had time to heal. The difference between the hydrophilic and hydrophobic cases, however, is striking. The layer of liquid in front of the hydrophobic wire is much thicker than that seen for the hydrophilic one, as shown in Fig. 2(c). Behind the wire, the liquid layer remains thin even at a high driving force. Moreover, when the driving force approaches its critical value, the liquid-solid interface around a hydrophilic wire assumes approximate axial symmetry. The symmetry is clearly broken around a hydrophobic wire since the thick body of liquid appears at any finite velocity.

Second, we consider the dynamics of the liquid water flowing around the wires. In order to understand the observed differences, it is imperative to note that hydrophilic and hydrophobic surfaces differ fundamentally in their wetting properties. For a hydrophilic wire, even a very small amount of liquid spontaneously covers the surface of the wire since water wets the surface. This thin layer may then flow around the wire, allowing the wire to move through the ice as liquid is produced by pressure melting in front of the wire at the same rate as it is consumed in solidification behind the wire [see Figs. 3(a) and 3(b)]. If, however, the wire is nonwetting, the liquid will seek to avoid the surface [see Figs. 3(c) and 3(d)]. In particular, the water will tend to form a finite wire-liquid-solid contact angle, so that all the liquid is in front of the wire in the high pressure region and there is solid ice behind the wire. As the pressure induced by the wire melts more water, a large liquid layer builds up. When the volume of liquid increases and the wire moves through it, the liquid will at some point also reach the top of the wire allowing it to finally pass the wire. The wire moves rather steadily also during liquid formation and thus there will be a region void of ice, left behind by the wire, for the liquid to fill and solidify in. (The liquid is denser than the solid.) This solidification depletes the liquid at the top of the wire, and another rapid liquid buildup phase follows before the next regelation burst. This qualitative difference between flow patterns around the hydrophilic and hydrophobic wires is quantitatively captured in the recorded water velocity fields. The flow of water is fastest directly at the sides of a hydrophilic wire [Fig. 3(e)], while for a hydrophobic wire the movement is the most rapid on top of the wire, due to the sudden surges of liquid into the voids left behind by the wire [Fig. 3(f)].

The observed behavior is somewhat counterintuitive: A hydrophobic surface in contact with water should move more easily than a hydrophilic one, since surface trapping and short slip lengths, leading to increased friction [36], are expected on a hydrophilic surface, but not on a hydrophobic one [37]. Here, however, hydrophobicity makes the wire resist water molecules from covering its surface and the remaining solid obstructs the liquid from moving around and past the wire. Therefore, a hydrophobic wire experiences more resistance to movement than a hydrophilic one.

The qualitatively different types of depinning transitions observed for the different wires can now be explained by the liquid morphology and flow patterns described above.



FIG. 3 (color online). (a) Schematic: The liquid flows easily around a wetting wire and only a thin layer of liquid builds. (b) Snapshot of a wetting wire, corresponding to (a). (c) Schematic: The liquid is slow to pass a nonwetting wire, leading to a thick liquid layer and formation of voids behind the wire. Once the liquid passes the wire, it rapidly fills the voids partially depleting the liquid layer. (d) Snapshots of a nonwetting wire, corresponding to (c). (e) Water velocity field around a wetting wire (in wire reference frame): the velocity is highest at the sides of the wire [red (dark gray), 0.1 Å/ps]. (f) Water velocity field around a nonwetting wire: the velocity is highest on top of the wire.
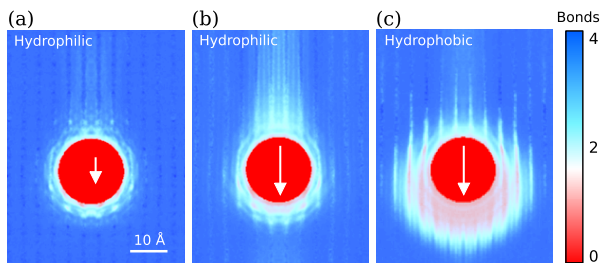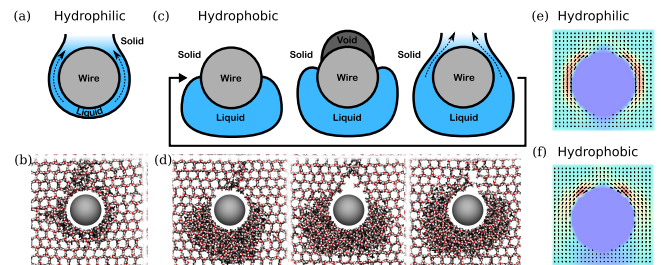


FIG. 2 (color online). (a) Average bonding energy (in the scale of the energy of ideal H bonds) of water molecules around a hydrophilic wire (9.0 Å radius) in the stick-slip regime. (b) Bonding in the sliding regime. (c) Bonding around a hydrophobic wire in the sliding regime. The direction of wire movement is downwards in each case. The vertical stripes are artifacts of the lattice structure of the surrounding ice.

For both hydrophilic and hydrophobic wires, there is at most a liquidlike premelt layer surrounding the wire in the stationary state. At depinning, the wire switches to a moving state, which for the hydrophilic case is similar to the stationary one, such that there is a thin, symmetric flow layer around the wire. Thus, the hydrophilic wire exhibits a continuous transition. The depinned state of the hydrophobic wire, on the other hand, includes an asymmetric layer of liquid comparable to the size of the wire, qualitatively distinct from the stationary state. Therefore, the depinning transition of the hydrophobic wire is discontinuous, and the hysteresis pattern seen in Fig. 1(b) is due to a delay in the development of the liquid layer.

The presented analysis is made for a nanowire, but it is also important to consider the validity of the arguments at the macroscopic limit. In this limit, any possible premelt layer of liquid around the wire, present in the stationary state, will be microscopic with respect to the wire (for layer width $d$ and radius $R$, $\lim d/R = 0$). A continuos depinning transition can be expected if such a layer is sufficient in providing a channel for the liquid to flow around the wire. If the wire is ideally wetting, any amount of liquid should spontaneously cover the wire, and this is indeed possible. If the wire is not fully wetting, one should expect a finite contact angle at the wire-liquid-solid interface, whereby the formation of a liquid layer of finite thickness ($\lim d/R > 0$) would be required for the liquid to fully surround the wire. In such a case, discontinuous depinning should occur.

In summary, we have used MD simulations of water and ice to demonstrate that the continuity of the depinning transition and symmetry of the water flow, including induced phase changes, depend on the hydrophilicity of the wire. Besides adding to the understanding of the general behavior of water, ice, and mechanical contacts with ice, the work has parallels to studies of flow in granular media and soft materials [38,39]. However, since the phenomenon of regelation is specific to water, the study describes a presumably unique property of water.

*teemu.hynninen@tut.fi

[1] J. G. Dash, A. W. Rempel, and J. S. Wettlaufer, Rev. Mod. Phys. **78**, 695 (2006).
[2] R. Rosenberg, Phys. Today **58**, No. 12, 50 (2005).
[3] M. Faraday, Proc. R. Soc. London **10**, 440 (1859).
[4] W. Gibbs, Trans. Conn. Acad. Arts Sci. **III**, 108 (1875).
[5] J. Weertman, J. Glaciol. **3**, 33 (1957).
[6] J. Thomson Bottomley, Proc. R. Soc. London **10**, 151 (1859).
[7] J. Thomson Bottomley, Nature (London) **5**, 185 (1872).
[8] J. F. Nye, Philos. Mag. **16**, 1249 (1967).
[9] L. D. Drake and R. L. Shreve, Proc. R. Soc. A **332**, 51 (1973).
[10] S. Tozuka and G. Wakahama, J. Phys. Chem. **87**, 4147 (1983).
[11] A. Michaelides and K. Morgenstern, Nature Mater. **6**, 597 (2007).
[12] J. Carrasco et al., Nature Mater. **8**, 427 (2009).
[13] Y. He et al., Nature Mater. **8**, 585 (2009).
[14] T. Fukuma et al., Phys. Rev. Lett. **104**, 016101 (2010).
[15] J. Matthiesen et al., Phys. Rev. Lett. **102**, 226101 (2009).
[16] M. Mehlhorn et al., Phys. Rev. Lett. **103**, 026101 (2009).
[17] K. Koga et al., Nature (London) **412**, 802 (2001).
[18] K. B. Jinesh and J. W. M. Frenken, Phys. Rev. Lett. **96**, 166103 (2006).
[19] K. B. Jinesh and J. W. M. Frenken, Phys. Rev. Lett. **101**, 036101 (2008).
[20] C. L. Dias et al., J. Chem. Phys. **131**, 054505 (2009).
[21] M. W. Mahoney and W. L. Jorgensen, J. Chem. Phys. **112**, 8910 (2000).
[22] C. L. Dias et al., Phys. Rev. Lett. **100**, 118101 (2008).
[23] K. A. T. Silverstein, A. D. J. Haymet, and K. A. Dill, J. Am. Chem. Soc. **120**, 3166 (1998).
[24] N. T. Southall and K. A. Dill, Biophys. Chem. **101–102**, 295 (2002).
[25] Moderate changes in $\varepsilon$ did not affect the conclusions. However, a very weakly attractive wire would resemble the hydrophobic case. A strongly attractive wire would not let the innermost layers of liquid leave its surface and regelate, effectively acting like a thicker wire.
[26] Other methods applied include a setup where a driving force acts on all water molecules, and a scheme where the wire is driven by an external force. Although changing the constraints affected the absolute values of forces needed to achieve certain wire velocities, the depinning behavior was qualitatively similar for all setups.
[27] M. Karttunen et al., Phys. Rev. Lett. **83**, 3518 (1999).
[28] L. Balents and M. P. A. Fisher, Phys. Rev. Lett. **75**, 4270 (1995).
[29] P. Chauve et al., Phys. Rev. B **62**, 6241 (2000).
[30] B. N. J. Persson, Sliding Friction: Theory and Applications (Springer, Berlin, 1998).
[31] F. P. Beer, E. R. Johnston, Jr., and J. T. Dewolf, Mechanics of Materials (McGraw-Hill, Boston, 2001), 3rd ed.
[32] P. C. Hohenberg and B. I. Halperin, Rev. Mod. Phys. **49**, 435 (1977).
[33] A. A. Middleton and D. S. Fisher, Phys. Rev. B **47**, 3530 (1993).
[34] Every bond is associated with a fractional value less than unity. In a liquid, the average bonding potential energy is only about half of that recorded in a perfect ice, even though the number of nearest neighbors is roughly four in both phases.
[35] J. R. Errington and P. G. Debenedetti, Nature (London) **409**, 318 (2001).
[36] M. H. Müser, L. Wenning, and M. O. Robbins, Phys. Rev. Lett. **86**, 1295 (2001).
[37] C. Sendner et al., Langmuir **25**, 10 768 (2009).
[38] A. N. Beris et al., J. Fluid Mech. **158**, 219 (1985).
[39] G. Ovarlez et al., Nature Mater. **9**, 115 (2010).